

Determination of the Maximum Velocity of a Peroxidase-like Nanozyme

Yuting Wang,[§] Tong Li,[§] and Hui Wei^{*}Cite This: <https://doi.org/10.1021/acs.analchem.3c01830>

Read Online

ACCESS |



Metrics & More

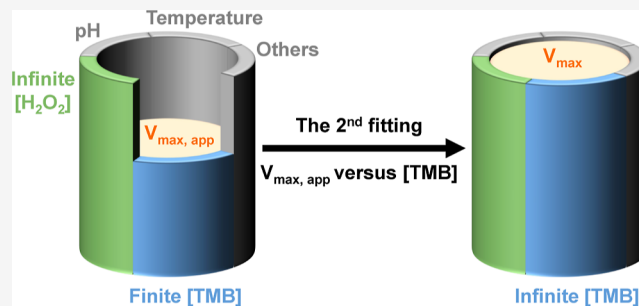


Article Recommendations



Supporting Information

ABSTRACT: Nanozymes are functional nanomaterials with enzyme-like activities, which have good stability and specific nanoscale properties. Among them, peroxidase-like (POD-like) nanozymes with two substrates are the biggest chunk and have been widely applied in biomedical and environmental fields. Maximum velocity (V_{\max}) is an essential kinetic parameter, accurate measurements of which can help in activity comparisons, mechanism studies, and nanozyme improvements. At present, the standardized assay determines the catalytic kinetics of POD-like nanozymes by a single fitting based on the Michaelis–Menten equation. However, the true V_{\max} cannot be confirmed by this method due to the test condition that the concentration of a fixed substrate is finite. Here, a double fitting method to determine the intrinsic V_{\max} of POD-like nanozymes is presented, which breaks through the limited concentration of the fixed substrate by an additional Michaelis–Menten fitting. Furthermore, a comparison of the V_{\max} among five typical POD-like nanozymes validates the accuracy and feasibility of our method. This work provides a credible method to determine the true V_{\max} of POD-like nanozymes, helping in activity comparisons and facilitating studies on the mechanism and development of POD-like nanozymes.



1. INTRODUCTION

Nanozymes, functional nanomaterials with enzyme-like activities, have grabbed much attention for their catalytic activities combined with unique nanoscale properties.^{1–4} They have been widely used in the fields of bioanalysis,^{5,6} medical diagnosis,^{7,8} therapeutics,^{9–11} and environmental protection.^{12,13} Among them, peroxidase-like (POD-like) nanozymes, which can catalyze the oxidation of reducing substrates by hydrogen peroxide (H_2O_2), have been studied most by far.^{14,15} Demand for kinetic assays of them has been increasing to accurately compare activities,^{16,17} deepen insights into catalytic mechanisms,^{18,19} and develop highly active POD-like nanozymes with improved application performances.^{20,21}

The kinetics of catalytic reactions is about variations of their initial velocities (V_0) versus reaction conditions like temperature, pH, and substrate concentration.²² Nanozymes exhibit similar catalytic kinetics to enzymes and V_0 as a function of the concentration of a substrate mostly obeys the Michaelis–Menten equation as follows

$$V_0 = V_{\max}[S]/(K_m + [S]) \quad (1)$$

Hence, to date, for kinetic assays of POD-like nanozymes that have two substrates, the standard method—we call it the “single fitting method”—is to first fix the limited concentration of one substrate, then measure V_0 with varying concentrations of the other substrate, and finally fit them using the Michaelis–Menten equation. Two kinetic parameters can be obtained,

including the Michaelis–Menten constant (K_m) and maximum velocity (V_{\max}).²³ V_{\max} is usually used to compare the activities of nanozymes. Obviously, two V_{\max} values can be obtained for a POD-like nanozyme separately for the two substrates using this method.

Since the V_0 of a POD-like nanozyme is positively correlated with the concentrations of the two substrates, theoretically, when concentrations of the two substrates are infinitely high, the V_0 is the true V_{\max} , which signifies that the two V_{\max} values for the two substrates are equal. However, the statistical analysis showed that the V_{\max} obtained by the single fitting method was different (Figure 1): we screened nearly 300 pieces of valid data on the two V_{\max} of POD-like nanozymes with commonly used 3,3',5,5'-tetramethylbenzidine (TMB) as the reducing substrate²⁴ and found that most of the differences between the two V_{\max} values were more than 10%—even nearly half of them exceeded 100%, which cannot be simply attributed to experimental errors. It was because of this that the fixed concentrations here were all finite, and the so-called V_{\max} would increase as they became higher. Therefore, such a V_{\max}

Received: April 27, 2023

Accepted: June 12, 2023

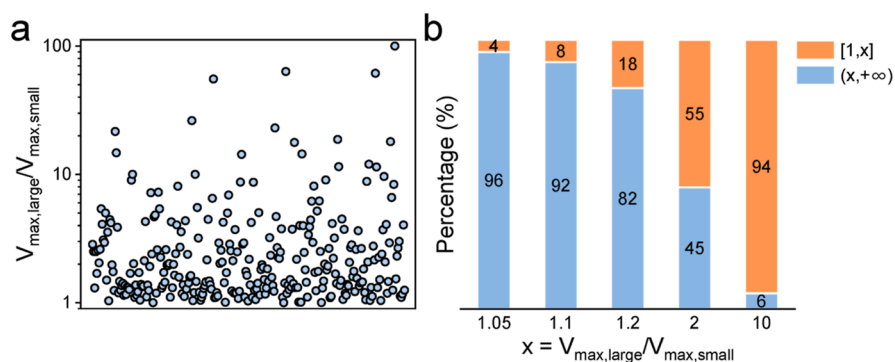


Figure 1. Statistics of V_{\max} values of POD-like nanozymes. (a) Distribution of ratios of the larger V_{\max} ($V_{\max,\text{large}}$) to the smaller one ($V_{\max,\text{small}}$). (b) Percentage of different ratios corresponding to (a). Data were collected from Google Scholar from January 1st to June 20th, 2022.

was more appropriately called an apparent maximum velocity ($V_{\max,\text{app}}$) since it was alterable, non-unique, and unable to reach the true maximum. Besides, further statistics revealed that various fixed concentrations were chosen in assays so that $V_{\max,\text{app}}$ could not be compared under the same conditions (Figure S1).

Herein, we propose a double fitting method that performs an additional Michaelis–Menten fitting on the basis of the single fitting method to break the limit of the finitely fixed substrate concentration and capture the intrinsic V_{\max} of the two-substrate reactions catalyzed by POD-like nanozymes. Using this method, the gaps between the two V_{\max} of five typical POD-like nanozymes—Prussian blue nanoparticles (PB NPs), PCN-222(Fe) (PCN = porous coordination network) NPs, Fe_3O_4 NPs, Pt NPs, and commercial graphene oxide (GO)—were almost always less than 10%, displaying its feasibility and universality. This method can not only help to compare activities but also study mechanisms and select nanozymes.

2. EXPERIMENTAL SECTION

2.1. Chemicals and Reagents. Potassium ferricyanide ($\text{K}_3[\text{Fe}(\text{CN})_6]$) was purchased from Nanjing Chemical Reagent Co., Ltd. Zirconium oxychloride octahydrate ($\text{ZrOCl}_2 \cdot 8\text{H}_2\text{O}$) was purchased from Energy Chemical. GO was purchased from XFANO Co., Ltd. Acetone was purchased from Shanghai Lingfeng Chemical Reagent Co., Ltd. Polyvinylpyrrolidone (PVP, $M_w = 2,4000$ Da), diethylene glycol (DEG), and 3,3',5,5'-tetramethylbenzidine dihydrochloride (TMB) were purchased from Aladdin. PVP (K30), hydrochloric acid (HCl), benzoic acid (BA), *N,N*-dimethylformamide (DMF), ferric chloride hexahydrate ($\text{FeCl}_3 \cdot 6\text{H}_2\text{O}$), trisodium citrate (Na_3Cit), anhydrous sodium acetate (NaAc), chloroplatinic acid ($\text{H}_2\text{PtCl}_6 \cdot 6\text{H}_2\text{O}$), acetate acid (HAc), and hydrogen peroxide (H_2O_2 , 30% wt) were purchased from Sinopharm Chemical Reagent Co., Ltd. Fe-TCPP [TCPP = tetrakis(4-carboxyphenyl)porphyrin] was synthesized as previously reported.²⁵ Deionized water was obtained from a Millipore Milli-Q system.

2.2. Preparation of Nanozymes. For PB NPs, in a typical procedure,²⁶ $\text{K}_3[\text{Fe}(\text{CN})_6]$ (263.4 mg) was dissolved in 80 mL of water in a 250 mL flask, followed by the addition of PVP (6 g, K30) under magnetic stirring until the solution is clear. Then, 80 mL of 10 mM HCl was added into the solution under magnetic stirring. Next, the solution was heated at 80 °C for 20 h without stirring. After cooling naturally to room temperature, PB NPs were obtained by centrifugation, washed

with ethanol and water three times each, and stored in water at 4 °C.

For PCN-222(Fe), in a typical procedure,²⁷ Fe-TCPP (20 mg), $\text{ZrOCl}_2 \cdot 8\text{H}_2\text{O}$ (60 mg), and BA (660 mg) were dissolved in 20 mL of DMF in a 50 mL flask by sonication. Then, the solution was heated at 90 °C for 5 h under mild stirring. After cooling naturally to room temperature, PCN-222(Fe) NPs were obtained by centrifugation, washed with DMF three times, and stored in DMF at 4 °C.

For Fe_3O_4 NPs, in a typical procedure,²⁸ $\text{FeCl}_3 \cdot 6\text{H}_2\text{O}$ (3 mmol) was dissolved in 30 mL of DEG under vigorous stirring, followed by the addition of Na_3Cit (1.2 mmol). The mixture was then heated at 80 °C under magnetic stirring for a clear solution. Next, after cooling to room temperature, anhydrous NaAc (9 mmol) was dissolved in the solution. The solution was sealed in a 50 mL Teflon-lined autoclave and heated at 200 °C for 6 h. After cooling naturally to room temperature, the solution was subjected to dialysis ($MWCO = 2000$ Da) for 3 days to obtain pure Fe_3O_4 NPs dispersed in water, which was stored at 4 °C.

For Pt NPs, in a typical procedure,²⁹ PVP (266 mg, $M_w = 24,000$ Da) was dissolved in 90 mL of methanol in a 250 mL flask under magnetic stirring, followed by the addition of 10 mL of 50 mM H_2PtCl_6 . The solution was then refluxed at 85 °C for 3 h under vigorous stirring. After cooling naturally to room temperature, the solution was subjected to rotary evaporation to remove methanol. Pt NPs were precipitated by acetone, redispersed in water, and stored at 4 °C.

2.3. Optimal pH Assay. Typically, for PB NPs, 100 μL of 80 $\mu\text{g mL}^{-1}$ NPs and 100 μL of 2 mM TMB were added into 1.7 mL of 0.2 M acetate buffer with different pH, followed by the introduction of 100 μL of 100 mM H_2O_2 . The final concentrations of NPs, TMB, and H_2O_2 were 4 $\mu\text{g mL}^{-1}$, 0.1 mM, and 5 mM, respectively. The absorption changes of the reaction solutions at 652 nm were monitored by a spectrophotometer. The initial velocities (V_0) were calculated based on the Beer–Lambert law. The curve of V_0 versus pH was plotted.

Similarly, for PCN-222(Fe), the final concentrations of NPs, TMB, and H_2O_2 were 1 $\mu\text{g mL}^{-1}$, 0.2 mM, and 5 mM, respectively. For Fe_3O_4 NPs, the final concentrations were 7 $\mu\text{g mL}^{-1}$, 2 mM, and 1 mM, respectively. For Pt NPs, the final concentrations were 0.043 $\mu\text{g mL}^{-1}$, 0.2 mM, and 5 mM, respectively. For GO, the final concentrations were 30 $\mu\text{g mL}^{-1}$, 0.8 mM, and 40 mM, respectively.

2.4. Kinetic Assay. Typically, for PB NPs, 100 μL of 80 $\mu\text{g mL}^{-1}$ PB NPs and 100 μL of TMB with concentrations from 2

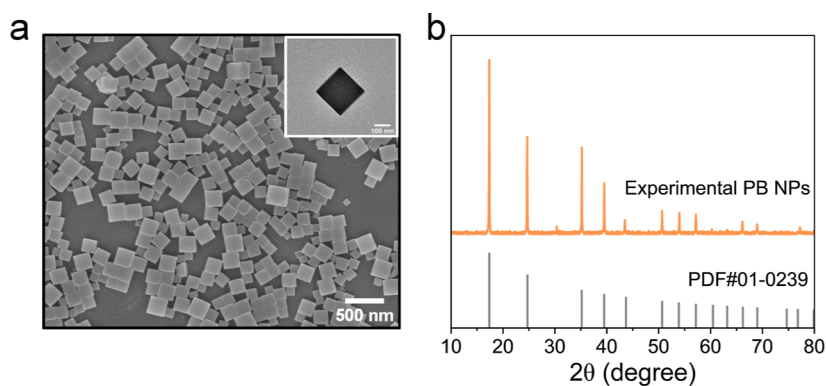


Figure 2. Characterizations of PB NPs. (a) Representative SEM image and TEM image (inset) and (b) XRD pattern of PB NPs.

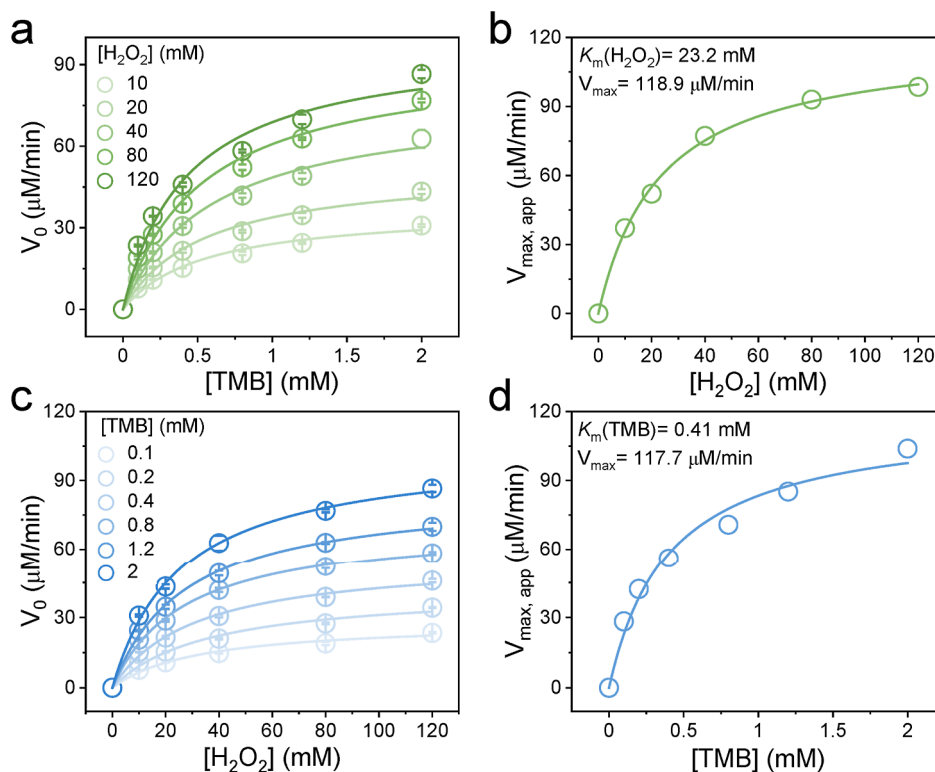


Figure 3. Kinetic study of PB NPs using the double fitting method based on the Michaelis–Menten equation. Plots of initial velocities (V_0) versus concentrations of (a) TMB and (c) H_2O_2 and their first fittings. Plots of apparent maximum velocities ($V_{max,app}$) obtained from (a,c) versus concentrations of (b) H_2O_2 and (d) TMB and their second fittings to obtain the intrinsic maximum velocities (V_{max}) and Michaelis constants (K_m). The concentration of PB NPs is $4 \mu\text{g/mL}$. The data are shown as means \pm SD ($n = 3$).

to 40 mM were added into 1.7 mL of 0.2 M acetate buffer (pH = 4), followed by the introduction of 100 μL of H_2O_2 with concentrations from 0.2 to 2.4 M. The final concentrations of PB NPs, TMB, and H_2O_2 were $4 \mu\text{g mL}^{-1}$, 0.1 to 2 mM, and 10 to 120 mM, respectively. The absorption changes of the reaction solutions at 652 nm were monitored by a spectrophotometer, and V_0 were calculated based on the Beer–Lambert law. To obtain the V_{max} for H_2O_2 [$V_{max}(H_2O_2)$], the plot of V_0 versus TMB concentrations from 0.1 to 2 mM was first fitted based on the Michaelis–Menten equation, respectively, under the conditions of five different H_2O_2 concentrations, obtaining five apparent maximum velocities for TMB [$V_{max,app}(TMB)$]. Then, the plot of $V_{max,app}(TMB)$ versus the corresponding H_2O_2 concentrations was fitted for the second time, obtaining the $V_{max}(H_2O_2)$.

2.5. Characterizations. The morphology of the nanozymes was obtained from a scanning electron microscope (Zeiss Ultra 55) and two transmission electron microscopes (FEI Tecnai F20 and JEOL 1400). The X-ray diffraction (XRD) patterns of nanozymes were obtained from an X-ray diffractometer (Rigaku Ultima). pH responses and kinetics of the nanozymes were studied by two UV–vis spectrophotometers (Agilent Carry 100 and Shimadzu UV-3600 Plus).

3. RESULTS AND DISCUSSION

PB NPs exhibit good POD-like activity, physicochemical properties, and biosafety for widespread utilization in the biomedical field^{30,31} and were used as a representative to study the double fitting method. PB NPs were fabricated as previously reported.²⁶ TEM and SEM confirmed the successful fabrication of PB NPs. The synthesized PB NPs exhibited a

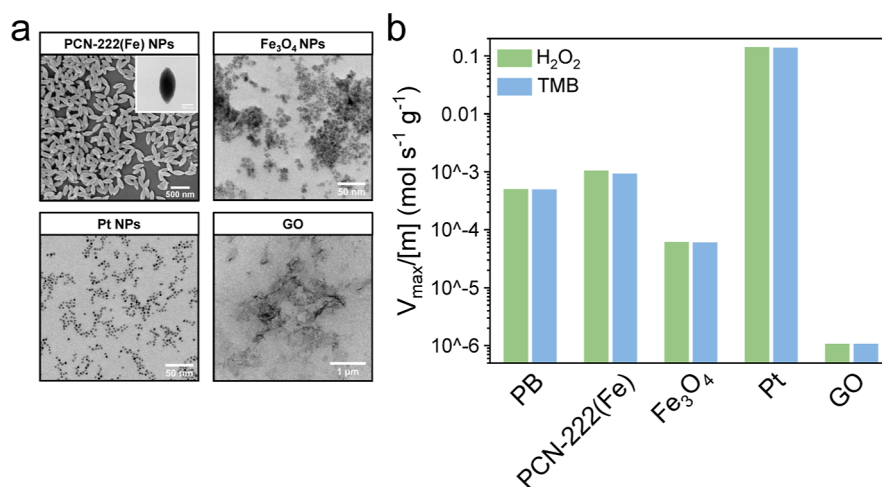


Figure 4. V_{\max} comparison between PB NPs and other nanozymes using the double fitting method. (a) Representative SEM and TEM images of other nanozymes. (b) Normalized V_{\max} for substrates H_2O_2 and TMB of the five typical POD-like nanozymes. $[m]$ is the mass concentration of a nanozyme used in the assay.

cubic morphology (Figure 2a). Furthermore, the XRD pattern of PB NPs was in accordance with a standard PDF card (Figure 2b).

To study the kinetics of PB NPs at an optimal pH, we first measured the V_0 of PB NPs at varying pHs. TMB was employed as the reducing substrate for the pH-response assay and the following kinetic study. The oxidized TMB has an absorption peak at 652 nm, which can be monitored by a spectrophotometer. As shown in Figure S2, PB NPs exhibited the best activity at pH 4, at which the kinetic assay of PB NPs was implemented.

According to our previous analysis, to obtain the true V_{\max} the core is to make the fixed substrate concentration infinitely high. If we could fit the V_0 versus the concentrations of H_2O_2 ($[H_2O_2]$) using the Michaelis–Menten equation with an infinitely high concentration of TMB ($[TMB]$), the obtained V_{\max} will be the true one for H_2O_2 [$V_{\max}(H_2O_2)$] and TMB [$V_{\max}(TMB)$] as well. Although we could not use an infinitely high $[TMB]$ in practical experiments, it is reasonable that the V_0 under the condition of a finite $[H_2O_2]$ and an infinitely high $[TMB]$ could be deemed as the $V_{\max,app}$ for TMB [$V_{\max,app}(TMB)$]. Based on the deduction, to obtain the $V_{\max}(H_2O_2)$ of PB NPs, we first measured and fitted V_0 versus $[TMB]$ employing different $[H_2O_2]$ from 10 to 120 mM separately to get five different $V_{\max,app}(TMB)$ with fixed $[H_2O_2]$ using the Michaelis–Menten equation (Figure 3a). The fitting in this step was called “the first fitting”. Afterward, the plot of the five $V_{\max,app}(TMB)$ versus the corresponding $[H_2O_2]$ was fitted using the Michaelis–Menten equation for a second time. As shown in Figure 3b, the second fitting succeeded, and the $V_{\max}(H_2O_2)$ was $118.9 \mu M \text{ min}^{-1}$.

Similarly, we measured the V_0 with varying $[H_2O_2]$ at various fixed $[TMB]$ from 0.1 to 2 mM and performed the first fitting, obtaining six $V_{\max,app}(H_2O_2)$ (Figure 3c). The six $V_{\max,app}(H_2O_2)$ and the corresponding $[TMB]$ were further applied to the second fitting. As shown in Figure 3d, the $V_{\max}(TMB)$ was $117.7 \mu M \text{ min}^{-1}$. The difference between the $V_{\max}(H_2O_2)$ and $V_{\max}(TMB)$ of PB NPs was around 1%, adopting the double fitting method, which verified the feasibility and accuracy of the method.

One thing to point out here is that we use the Michaelis–Menten equation for fitting rather than its double-reciprocal

form called “Lineweaver–Burk equation”. By using MATLAB to simulate input perturbations for fitting, we found that the Michaelis–Menten equation had a better anti-interference performance (Supporting Information). The fitting method may have a substantial effect on the results of kinetic assays, and the Michaelis–Menten equation could be a better choice by far.

Finally, to validate the universality of the double fitting method, we prepared another four classic POD-like nanozymes, including PCN-222(Fe) NPs, Fe_3O_4 NPs, Pt NPs, and GO. The morphologies and successful fabrication of them were confirmed by TEM images, SEM images, and XRD patterns (Figures 4a and S3). Using the same method, we assayed their kinetics at the optimal pH and the results showed their intrinsic V_{\max} (Figure S4–S8). For three of them, the differences between the two V_{\max} were less than 5%. However, the difference of PCN-222(Fe) was slightly more than 10%. Hence, the double fitting method could be widely applied for the kinetic study of POD-like nanozymes. In addition, activity comparison is one of the main purposes of the kinetic study. Mass activity is widely used for enzymes and also a useful parameter for nanozymes in certain applications.³² Hence, we compared the activities of the nanozymes using mass activity. Considering that various mass concentrations of the nanozymes were employed during the measurement of the V_{\max} , we divided the V_{\max} by the mass concentrations of the nanozymes for activity comparison. As shown in Figure 4b, Pt NPs exhibited a much higher activity than that of the other four nanozymes at an identical mass concentration. So, this method can be used for activity comparison effectively.

4. CONCLUSIONS

To sum up, we have introduced the double fitting method of kinetic assays to determine the true V_{\max} of various POD-like nanozymes, which added an additional Michaelis–Menten fitting based on the single fitting method to break the limitation of finitely fixed substrate concentrations. The accuracy and practicability of this method were demonstrated by five typical POD-like nanozymes for their activity comparison. Along with activity comparisons, this work will facilitate the mechanism studies and activity improvements of POD-like nanozymes.

■ ASSOCIATED CONTENT

SI Supporting Information

The Supporting Information is available free of charge at <https://pubs.acs.org/doi/10.1021/acs.analchem.3c01830>.

XRD patterns, optimal pH measurement, kinetic measurement, and discussion of fitting methods (PDF)
Papers used for statistics (XLSX)

■ AUTHOR INFORMATION

Corresponding Author

Hui Wei – College of Engineering and Applied Sciences, Nanjing National Laboratory of Microstructures, Jiangsu Key Laboratory of Artificial Functional Materials and State Key Laboratory of Analytical Chemistry for Life Science, School of Chemistry and Chemical Engineering, Chemistry and Biomedicine Innovation Center (ChemBIC), Nanjing University, Nanjing, Jiangsu 210023, China; orcid.org/0000-0003-0870-7142; Email: weihui@nju.edu.cn

Authors

Yuting Wang – College of Engineering and Applied Sciences, Nanjing National Laboratory of Microstructures, Jiangsu Key Laboratory of Artificial Functional Materials, Nanjing University, Nanjing, Jiangsu 210023, China

Tong Li – College of Engineering and Applied Sciences, Nanjing National Laboratory of Microstructures, Jiangsu Key Laboratory of Artificial Functional Materials, Nanjing University, Nanjing, Jiangsu 210023, China

Complete contact information is available at: <https://pubs.acs.org/10.1021/acs.analchem.3c01830>

Author Contributions

[§]Y.W. and T.L. contributed equally to this work.

Notes

The authors declare no competing financial interest.

■ ACKNOWLEDGMENTS

This work was funded by the National Key R&D Program of China (2019YFA0709200 and 2021YFF1200700), the National Natural Science Foundation of China (21874067 and 21722503), Jiangsu Provincial Key R&D Program (BE2022836), the PAPD Program, and the Fundamental Research Funds for the Central Universities (202200325 and 021314380195).

■ REFERENCES

- (1) Wei, H.; Wang, E. *Chem. Soc. Rev.* **2013**, *42*, 6060–6093.
- (2) Wei, H.; Gao, L.; Fan, K.; Liu, J.; He, J.; Qu, X.; Dong, S.; Wang, E.; Yan, X. *Nano Today* **2021**, *40*, 101269.
- (3) Zhang, R.; Yan, X.; Fan, K. *Acc. Mater. Res.* **2021**, *2*, 534–547.
- (4) Fan, K.; Gao, L.; Wei, H.; Jiang, B.; Wang, D.; Zhang, R.; He, J.; Meng, X.; Wang, Z.; Fan, H.; Wen, T.; Duan, D.; Chen, L.; Jiang, W.; Lu, Y.; Jiang, B.; Wei, Y.; Li, W.; Yuan, Y.; Dong, H.; Zhang, L.; Hong, C.; Zhang, Z.; Cheng, M.; Geng, X.; Hou, T.; Hou, Y.; Li, J.; Tang, G.; Zhao, Y.; Zhao, H.; Zhang, S.; Xie, J.; Zhou, Z.; Ren, J.; Huang, X.; Gao, X.; Liang, M.; Zhang, Y.; Xu, H.; Qu, X.; Yan, X. *Prog. Chem.* **2023**, *35*, 1–87.
- (5) Wei, H.; Wang, E. *Anal. Chem.* **2008**, *80*, 2250–2254.
- (6) Xi, Z.; Wei, K.; Wang, Q.; Kim, M. J.; Sun, S.; Fung, V.; Xia, X. *J. Am. Chem. Soc.* **2021**, *143*, 2660–2664.
- (7) Ding, H.; Cai, Y.; Gao, L.; Liang, M.; Miao, B.; Wu, H.; Liu, Y.; Xie, N.; Tang, A.; Fan, K.; Yan, X.; Nie, G. *Nano Lett.* **2019**, *19*, 203–209.
- (8) Liu, D.; Ju, C.; Han, C.; Shi, R.; Chen, X.; Duan, D.; Yan, J.; Yan, X. *Biosens. Bioelectron.* **2021**, *173*, 112817.
- (9) Yang, J.; Zhang, R.; Zhao, H.; Qi, H.; Li, J.; Li, J.-F.; Zhou, X.; Wang, A.; Fan, K.; Yan, X.; Zhang, T. *Exploration* **2022**, *2*, 20210267.
- (10) Zhu, D.; Chen, H.; Huang, C.; Li, G.; Wang, X.; Jiang, W.; Fan, K. *Adv. Funct. Mater.* **2022**, *32*, 2110268.
- (11) Cao, F.; Jin, L.; Gao, Y.; Ding, Y.; Wen, H.; Qian, Z.; Zhang, C.; Hong, L.; Yang, H.; Zhang, J.; Tong, Z.; Wang, W.; Chen, X.; Mao, Z. *Nat. Nanotechnol.* **2023**, *18*, 617–627.
- (12) Natalio, F.; André, R.; Hartog, A. F.; Stoll, B.; Jochum, K. P.; Wever, R.; Tremel, W. *Nat. Nanotechnol.* **2012**, *7*, 530–535.
- (13) Jiang, S.; Su, G.; Wu, J.; Song, C.; Lu, Z.; Wu, C.; Wang, Y.; Wang, P.; He, M.; Zhao, Y.; Jiang, Y.; Zhao, X.; Rao, H.; Sun, M. *ACS Appl. Mater. Interfaces* **2023**, *15*, 11787–11801.
- (14) Gao, L.; Zhuang, J.; Nie, L.; Zhang, J.; Zhang, Y.; Gu, N.; Wang, T.; Feng, J.; Yang, D.; Perrett, S.; Yan, X. *Nat. Nanotechnol.* **2007**, *2*, 577–583.
- (15) Li, S.; Zhou, Z.; Tie, Z.; Wang, B.; Ye, M.; Du, L.; Cui, R.; Liu, W.; Wan, C.; Liu, Q.; Zhao, S.; Wang, Q.; Zhang, Y.; Zhang, S.; Zhang, H.; Du, Y.; Wei, H. *Nat. Commun.* **2022**, *13*, 827.
- (16) Ji, S.; Jiang, B.; Hao, H.; Chen, Y.; Dong, J.; Mao, Y.; Zhang, Z.; Gao, R.; Chen, W.; Zhang, R.; Liang, Q.; Li, H.; Liu, S.; Wang, Y.; Zhang, Q.; Gu, L.; Duan, D.; Liang, M.; Wang, D.; Yan, X.; Li, Y. *Nat. Catal.* **2021**, *4*, 407–417.
- (17) Deng, Y.; Gao, Y.; Li, T.; Xiao, S.; Adeli, M.; Rodriguez, R. D.; Geng, W.; Chen, Q.; Cheng, C.; Zhao, C. *ACS Nano* **2023**, *17*, 2943–2957.
- (18) Komkova, M. A.; Ibragimova, O. A.; Karyakina, E. E.; Karyakin, A. A. *J. Phys. Chem. Lett.* **2021**, *12*, 171–176.
- (19) Ma, C.; Xu, Y.; Wu, L.; Wang, Q.; Zheng, J.-J.; Ren, G.; Wang, X.; Gao, X.; Zhou, M.; Wang, M.; Wei, H. *Angew. Chem., Int. Ed.* **2022**, *61*, No. e202116170.
- (20) Razlivina, J.; Serov, N.; Shapovalova, O.; Vinogradov, V. *Small* **2022**, *18*, 2105673.
- (21) Wei, Y.; Wu, J.; Wu, Y.; Liu, H.; Meng, F.; Liu, Q.; Midgley, A. C.; Zhang, X.; Qi, T.; Kang, H.; Chen, R.; Kong, D.; Zhuang, J.; Yan, X.; Huang, X. *Adv. Mater.* **2022**, *34*, 2201736.
- (22) Robinson, P. K. *Essays Biochem.* **2015**, *59*, 1–41.
- (23) Jiang, B.; Duan, D.; Gao, L.; Zhou, M.; Fan, K.; Tang, Y.; Xi, J.; Bi, Y.; Tong, Z.; Gao, G. F.; Xie, N.; Tang, A.; Nie, G.; Liang, M.; Yan, X. *Nat. Protoc.* **2018**, *13*, 1506–1520.
- (24) Zhang, X.; Yang, Q.; Lang, Y.; Jiang, X.; Wu, P. *Anal. Chem.* **2020**, *92*, 12400–12406.
- (25) Feng, D.; Gu, Z.; Li, J.; Jiang, H.; Wei, Z.; Zhou, H. *Angew. Chem., Int. Ed.* **2012**, *51*, 10307–10310.
- (26) Li, J.; Liu, X.; Tan, L.; Cui, Z.; Yang, X.; Liang, Y.; Li, Z.; Zhu, S.; Zheng, Y.; Yeung, K. W. K.; Wang, X.; Wu, S. *Nat. Commun.* **2019**, *10*, 4490.
- (27) Park, J.; Jiang, Q.; Feng, D.; Mao, L.; Zhou, H. *J. Am. Chem. Soc.* **2016**, *138*, 3518–3525.
- (28) Shen, L.; Bao, J.; Wang, D.; Wang, Y.; Chen, Z.; Ren, L.; Zhou, X.; Ke, X.; Chen, M.; Yang, A. *Nanoscale* **2013**, *5*, 2133–2141.
- (29) Liu, Y.; Cheng, Y.; Zhang, H.; Zhou, M.; Yu, Y.; Lin, S.; Jiang, B.; Zhao, X.; Miao, L.; Wei, C.; Liu, Q.; Lin, Y.; Du, Y.; Butch, C. J.; Wei, H. *Sci. Adv.* **2020**, *6*, No. eabb2695.
- (30) Komkova, M. A.; Karyakin, A. A. *Microchim. Acta* **2022**, 189, 290.
- (31) Lu, K.; Zhu, X.; Li, Y.; Gu, N. *J. Mater. Chem. B* **2023**, DOI: 10.1039/D2TB02617A.
- (32) Zandieh, M.; Liu, J. *Adv. Mater.* **2023**, 2211041.